Magnetic memory effect in type-II superconductor/ferromagnet bilayers

2014 Supercond. Sci. Technol. 27 055024

(http://iopscience.iop.org/0953-2048/27/5/055024)

IOP Publishing Superconductor Science and Technology
Supercond. Sci. Technol. **27** (2014) 055024 (9pp) doi:10.1088/0953-2048/27/5/055024

Magnetic memory effect in type-II superconductor/ferromagnet bilayers

S L Prischepa[1], M Yu Kupriyanov[2], C Cirillo[3] and C Attanasio[3]

[1] Belarusian State University of Informatics and Radioelectronics, P Browka 6, Minsk 220013, Belarus
[2] Skobeltsyn Institute of Nuclear Physics, Moscow State University, Moscow 119992, Russia and Moscow Institute of Physics and Technology, Dolgoprudny, Moscow 141700, Russia
[3] CNR-SPIN Salerno and Dipartimento di Fisica 'E R Caianiello', Università degli Studi di Salerno, Fisciano (Sa) I-84084, Italy

E-mail: attanasio@sa.infn.it

Received 18 November 2013, revised 11 February 2014
Accepted for publication 14 February 2014
Published 27 March 2014

Abstract

We study the temperature dependence of the critical current density, $J_c^{S/F}(T)$, of a Nb/PdNi (PdNi = $Pd_{84}Ni_{16}$) bilayer before and after the application of a magnetic field oriented either out-of-the-plane or in-the-plane of the substrate. Nb and PdNi layers interact through both electromagnetic and proximity coupling. The values of $J_c^{S/F}$ strongly depend on the magnetic history of the samples. Indeed, the $J_c^{S/F}$ values measured when the PdNi is in the out-of-plane remanent state are reduced by a factor of two, in the whole investigated temperature range, compared to the case when the PdNi is in the demagnetized state. This behavior can be accounted for by the out-of-plane magnetocrystalline anisotropy of the PdNi layer producing stray fields which, in turn, can induce a spontaneous vortex phase in the Nb layer. The topology of these vortices is strongly modified by the proximity coupling as confirmed by theoretical calculations. The $J_c^{S/F}$ values are only weakly affected by the in-plane remanence of the PdNi layer.

Keywords: interplay superconductivity and magnetism, proximity effect, electromagnetic coupling, S/F hybrids

(Some figures may appear in colour only in the online journal)

1. Introduction

Interplay between superconductivity and ferromagnetism has been intensively studied during the last years. In thin film based heterostructures these two antagonistic orderings interact with each other in two ways: by the long range, but weaker, electromagnetic coupling (EC) [1, 2] and by the short range, but stronger, proximity coupling, namely the proximity effect (PE) [3]. Due to its weakness EC can be profitably investigated depositing a thin insulating film between the S- and the F-layer, thus preventing the occurrence of PE. In this configuration interaction between vortices in a type-II superconductor and the intense stray fields from a ferromagnet, can effectively govern the superconducting properties of the system. The effect can be exploited for the realization, for example, of nonvolatile superconducting valves [4–8], and for tuning the vortex confinement and pinning [9–11]. Moreover, the stray fields of the ferromagnetic layer can strongly modify the vortex state in the superconducting film, leading to the nucleation of the spontaneous vortex phase in the absence of any external applied magnetic field [12–14], as recently observed in Nb/Py bilayers by means of low-temperature magnetic force microscopy [15]. The topology of these spontaneous vortices depends on several parameters, as, for instance, the relation between the thickness, d_S, and the magnetic field penetration depth, λ, of the superconducting film, as well as the easy-axis of magnetization of the F-layer. If one restricts to the case of thin S-layers, $d_S \ll \lambda$, and supposing that the easy-axis of magnetization is oriented out-of-plane, it results that straight vortices are induced in the superconductor [13].

Concerning the consequences of the exchange interaction on the current-carrying capability, it is well established

[16, 17] that PE produces a strong reduction of the critical current density in S/F hybrids, $J_c^{S/F}$, due to the suppression of the order parameter inside the superconductor. Moreover, PE has also important consequences on the vortex topology, since close to the S/F interface the superconducting correlations are suppressed in F, namely the superconducting coherence length ξ_S diverges and the vortex shape can change. From the point of view of the critical current density values, one could assimilate the S/F bilayer to a homogeneous superconducting film exposed to an equivalent external magnetic field [18]. However, in the previous works focusing on the study of $J_c^{S/F}$ [16, 17] the influence of the real domain structure of the F-layer, which can generate for instance stray fields piercing the superconductor, as well as a systematic study of the dependence of the critical current density on the magnetic history of the sample were not explored.

In contrast, the influence of the stray fields was deeply investigated in proximity coupled S/F hybrids both in bilayers [19–21] as well as in spin valve [22] structures mainly by magnetoresistive measurements. Moreover, an inverse proximity effect was recently invoked to explain the anomalous field dependence of the superconducting critical current in proximity coupled bilayers based on a half-metallic ferromagnet [23]. Finally, in systems combining oxide ferromagnets and superconductors [24] memory effects controlled by magnetic anisotropy were found [25].

In this work we study the transport properties of a Nb/PdNi bilayer taking into account both the contributions of the PE and EC. The former acts as an equivalent field and does not depend on the magnetic history of the sample. On the other hand, EC, caused by the stray fields originated from the F-layer, due to the peculiar magnetic anisotropy of the PdNi layer, can produce a stronger suppression of $J_c^{S/F}$, which is highly dependent of the preparation state of the sample, thus making it possible to control the vortex topology and the pinning strength in the system. To demonstrate this, the temperature dependence on $J_c^{S/F}$ was measured for different magnetic configurations of the PdNi layer, namely in the virgin (demagnetized, D) state, and both in the parallel (in-plane) and perpendicular (out-of-plane) remanent states (IPR and OPR, respectively). The latter were obtained applying an intense magnetic field (larger than the saturation value) for both the orientations. The experimental data show that the $J_c^{S/F}$ values strongly depend on the magnetic history. Indeed, we show that a spontaneous vortex phase is induced in Nb when the PdNi layer is in the OPR state. In this case the values of $J_c^{S/F}$ are considerably lower than those measured in the D state. Moreover, the vortex topology differs from that present in a single Nb film. In particular, the vortex diameter is larger due to the modulation of the internal magnetization of PdNi layer caused, in turn, by the vortices in the Nb layer. The increased in-plane dimensions of vortices enhances their mobility and, consequently, depress the critical current density values. The proximity additionally increases the vortex diameter close to the S/F interface thus leading to an even weaker pinning. This effect is less pronounced measuring in the IPR state. The values of $J_c^{S/F}$ measured after warming the sample above the Curie temperature, T_{Curie}, fully revert to the ones initially obtained in the D state. Finally, it is worth noticing that the possibility to control the pinning regimes is a S/F system coupled by exchange interaction via the stray fields of the ferromagnet is not straightforward, the success of the experiment essentially lying in the suitable choice of the ferromagnetic material.

2. Experimental details

The Nb/PdNi (PdNi = $Pd_{84}Ni_{16}$) bilayer was sputtered on Si(100) substrates in an ultra-high-vacuum system at an Ar pressure of 0.13 Pa [26]. Typical deposition rates were 0.28 nm s^{-1} for Nb and 0.40 nm s^{-1} for PdNi. The Ni concentration in the Nb/PdNi films was estimated by energy dispersion spectrometry analyses. The thicknesses of Nb and PdNi (d_F) layers were equal, $d_S = d_F = 30$ nm. Using a lift-off procedure samples were patterned into stripes $w = 20$ μm wide and $l = 300$ μm long. The critical temperature, T_c, of the patterned bilayer was 6.0 K. For comparison a single Nb film 30-nm thick, patterned into a bridge with the same dimensions, was also investigated. The critical temperature and the low-temperature resistivity of this reference film were $T_c = 7.3$ K and $\rho_S = 17$ $\mu\Omega$ cm, respectively.

I–V characteristics were recorded using a pulsed technique in a standard four-probe geometry [26]. $J_c^{S/F}$ values were extracted from the critical current values, considering only the cross-section of the Nb layer, namely $J_c^{S/F} = I_c/wd_{Nb}$. Here I_c was determined according to the voltage criterion of $V_c = 1$ μV (corresponding to the electric field criterion $E_c = 3.33$ mV m^{-1}). Magnetic properties of the PdNi alloy were studied on unpatterned 19-nm thick single film with a slightly different Ni percentage ($Pd_{81}Ni_{19}$) with respect to the one present in the bilayer[4]. The magnetization hysteresis loops for PdNi single films were measured by SQUID magnetometry at $T = 10$ K for magnetic fields applied both parallel and perpendicular to the surface of the sample. Magnetoresistance measurements of $Pd_{81}Ni_{19}$ bridges (not shown here) were also measured to exclude possible differences in the hysteretic behavior between unstructured and structured samples. Concerning the domain structure of the patterned sample, it is worth underlining that the out-of-plane magnetization configuration of PdNi micrometric structures was also confirmed in [28].

3. Results

The magnetization loops $M(H)$ of a single $Pd_{81}Ni_{19}$ film ($d_F = 19$ nm), measured for both the perpendicular (open symbols) and parallel (closed symbols) orientations of the applied magnetic field, are shown in figure 1. Data are normalized to the saturation values M^{sat}, which were equal to 24.8 (20.6) emu g^{-1} for the perpendicular (parallel) configuration. Both the squareness of the hysteresis loop, M^{rem}/M^{sat}, (M^{rem}

[4] The ferromagnetic properties of $Pd_{81}Ni_{19}$ are very similar to those of $Pd_{84}Ni_{16}$. In particular, the exchange energy, E_{ex}, changes from 15 meV for $Pd_{84}Ni_{16}$ [26] to 20 meV for $Pd_{81}Ni_{19}$, and T_{Curie} varies from 190 to 210 K [27].

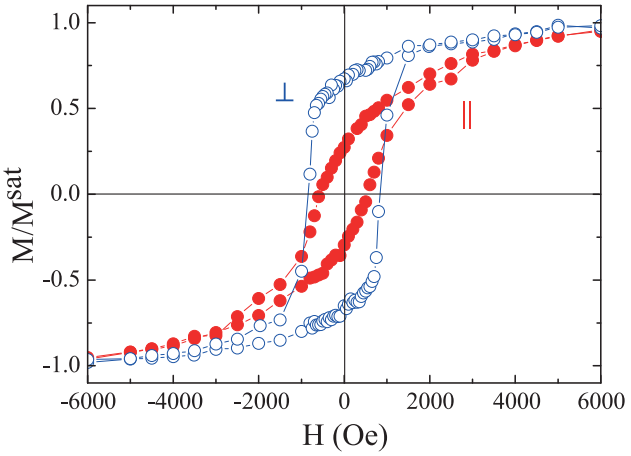

Figure 1. Magnetic hysteresis loops for a $Pd_{81}Ni_{19}$ film 19-nm thick measured at $T = 10$ K. Open (closed) symbols correspond to the perpendicular (parallel) orientation of the applied magnetic field with respect to the substrate surface.

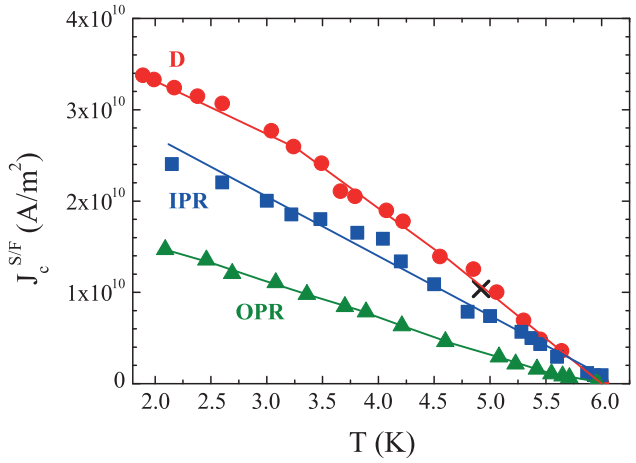

Figure 2. $J_c^{S/F}(T)$ behavior for the Nb/PdNi bilayer. Data obtained in the demagnetized, OPR and IPR states are shown respectively as circles, triangles and squares. The lines are guides to the eye. The cross corresponds to the measurement performed at $T = 4.9$ K after the sample has been warmed above the PdNi Curie temperature.

indicates the magnetization in the remanent state) and the coercivity, H^{coerc}, are larger for the perpendicular orientation. In particular, for the perpendicular case $(M^{rem}/M^{sat})_{\perp} \approx 0.7$ and $H_{\perp}^{coerc} = 870$ Oe, while for the parallel configuration $(M^{rem}/M^{sat})_{\parallel} \approx 0.3$ and $H_{\parallel}^{coerc} = 520$ Oe. It follows that the sample has an out-of-plane easy-axis of magnetization, namely the magnetocrystalline anisotropy dominates the shape anisotropy even in a very thin PdNi film. The out-of-plane anisotropy is indeed a characteristic of Pd_xNi_{1-x} films [28], as well as of similar dilute alloys such as Cu_xNi_{1-x} [29]. Finally, the saturation field H^{sat} is around 6 kOe for both the orientations. From the M^{rem} values it is also possible to evaluate the amplitude of the stray field of PdNi layer in remanent state. Assuming that the main contribution to the magnetic moment comes from Ni atoms it is $M_{\perp}^{rem} \approx$ 1900 G and $M_{\parallel}^{rem} \approx 680$ G. The temperature dependence of the remanent magnetization for the same film is reported in the inset of figure 2 of [27].

Figure 2 shows the behavior of $J_c^{S/F}(T)$ of the Nb/PdNi bilayer. Results refer to four sets of measurements performed following different magnetization procedures. The first set was obtained measuring $J_c^{S/F}(T)$ cooling the virgin sample from room temperature in the absence of any external magnetic field, so the PdNi layer was in the D state (circles). For the second set, the sample was warmed above the PdNi Curie temperature, $T_{Curie} \approx 190$ K [26], and then cooled down to $T = 4.2$ K when a perpendicular magnetic field of 25 kOe, well above the H^{sat} value, was applied in order to magnetize the PdNi layer. Finally, the field was switched off (OPR) and $J_c^{S/F}(T)$ was recorded (triangles). For the third set of measurements, the sample was first warmed up to room temperature, then cooled down to $T = 4.2$ K and then a parallel magnetic field of 25 kOe was applied, in such a way that the magnetization of the PdNi layer was always perpendicular to the stripe length. Critical current measurements with the magnetic field applied parallel to the stripe were not performed, since we do not expect any effect relevant for the analyzed experiment, considering that the magnetic domains are significantly smaller compared to the bridge width (see the following section for more details). Finally, the field was switched off (IPR) and $J_c^{S/F}(T)$ was acquired (squares). The final measurement was recorded after warming the sample up to room temperature and then cooling it down to $T = 4.9$ K (cross). Note that after each magnetization procedure the sample was brought to $T > T_c$ to avoid the possible presence of trapped flux in the Nb layer. The main result of this work, which will be discussed in detail in the following sections, is the strong reduction of $J_c^{S/F}(T)$ (by more than a factor of two) in the entire temperature range in the OPR state with respect to the D state. On the other hand, when the PdNi layer is in the IPR state the $J_c^{S/F}(T)$ reduction is noticeably smaller and limited to temperatures lower than $T \approx 5.25$ K.

4. Discussion

In this work both the electromagnetic [12] and the proximity [18] coupling were taken into account to explain the behavior of $J_c^{S/F}(T)$ shown in figure 2. The proximity coupling, which does not depend on the orientation of the external magnetic field, is mainly determined by scalar quantities such as the exchange energy of the ferromagnet, E_{ex}, the T_c of the superconductor, the diffusion coefficients and resistivities of both materials, as well as by the S/F interface transparency. On the other hand, the effects of the electromagnetic coupling, namely the conditions for the vortex phase nucleation, strongly depend on the direction of the magnetic field experienced by the S-layer. In the following we discuss how the vortex properties of the Nb layer are affected by the magnetic configuration of the PdNi, starting with the demagnetized and the OPR state in section 4.1 and then considering the IPR state in section 4.2.

4.1. Demagnetized and OPR state

In the demagnetized state the PdNi layer is in a multidomain state of average diameter around 100 nm [28, 30], whose

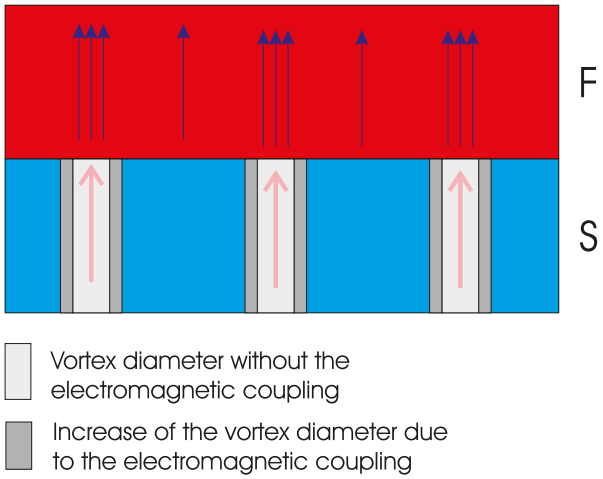

Figure 3. Schematic (not in scale) representation of the magnetic state and vortex arrangement in the Nb/PdNi bilayer. The easy-axis of magnetization in PdNi is out-of-plane. In this case only the electromagnetic coupling is considered for simplicity and the condition $H^{\rm stray} > H_{\rm c1}$ is supposed. Vortices in the S-layer are perpendicular to the sample surface and parallel to each other. The intensity of the magnetic field in the F-layer is larger in the correspondence of the vortex in S causing the suppression of the superconducting correlations in the vortex region. This fact increases the vortex diameter.

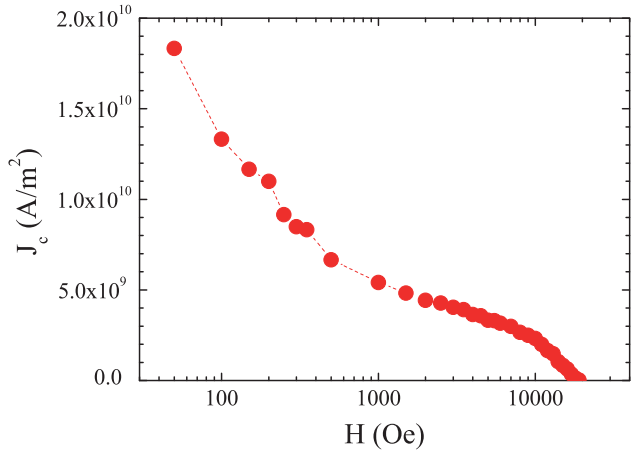

Figure 4. $J_{\rm c}^{S}(H)$ for a single Nb film 30-nm thick at $T = 4.2$ K. The magnetic field is perpendicular to the substrate surface.

magnetization is randomly oriented along the easy-axis, that is out-of-plane, as shown in the previous section. Therefore in this configuration the superconducting layer is exposed to antiparallel stray fields which can create antiparallel vortices oriented out-of-plane [15], provided that they exceed the first critical magnetic field of the S-layer (see the discussion that follows). When the Lorentz force is larger the local pinning force vortices start to move towards each other and annihilate over the domain walls. As a result, in this case the effect of the electromagnetic coupling is negligible, and it would be completely absent if the stray fields were too low to induce vortices in the S-layer. Therefore in the D state the values of $J_{\rm c}^{\rm S/F}$ are depressed compared to those of a single Nb film of the same thickness only due to the proximity effect. This situation was investigated for the same Nb/PdNi bilayer in [17], where, however, the effect of the magnetic history of the F-layer on $J_{\rm c}^{\rm S/F}$ was not explored. In that work, due to the suppression of the superconducting order parameter in the S-layer in contact with the ferromagnet, $J_{\rm c}^{\rm S/F}$ was strongly depressed compared to the single Nb film (almost as a factor of two at $t = 0.56$). Moreover, analyzing the magnetic field dependence of the critical current density of the single Nb film, $J_{\rm c}^{\rm S}(H)$, at $t = 0.56$ it can be inferred that the proximity effect depressed the critical current as an external magnetic field of 50 Oe was applied perpendicularly to the sample surface [17]. On the other hand, in the OPR state the PdNi is almost saturated due to the large remanence in this orientation ($M_{\perp}^{\rm rem} \approx 0.7 M_{\perp}^{\rm sat}$). According to the results of [31], the shape of our loop justifies the presence of strong disorder, which usually prevents easy inversion of the magnetization. Therefore, it is reasonable to assume that in the OPR state the sample is almost in a single domain configuration. Consequently, the S-layer experiences an effective perpendicular field which could create vortices oriented perpendicularly to the sample surface, see figure 3. In this situation the values of $J_{\rm c}^{\rm S/F}(T)$ will be determined not only by the proximity effect, but also by the motion of these spontaneous vortices. Generally, spontaneous vortices in the S-layer are created when the magnetic moment of the F-layer is of the order of $H_{\rm c1}$, the lower critical magnetic field of the superconductor [32]. The value of $H_{\rm c1}$ can be estimated from the expression $H_{\rm c1} = \Phi_0/4\pi\lambda_{\perp}^2$ [33], where Φ_0 is the flux quantum and $\lambda_{\perp}$ is the magnetic field penetration depth. For our 30-nm thick Nb film $\lambda_{\perp}$ can be estimated to be around 120 nm [34] so $H_{\rm c1} \approx 115$ Oe. This value is much lower than the stray field generated by a bare PdNi layer in the OPR state estimated in section 3, $M_{\perp}^{\rm rem} \approx 1900$ G. However, the field experienced by the S-layer in contact with the ferromagnet can, in principle, be different from $M_{\perp}^{\rm rem}$ and, actually, it cannot be directly measured. Nevertheless, the equivalent stray field in the OPR state can again be estimated by comparing $J_{\rm c}^{\rm S/F}$ with the critical current density of a single Nb film in the presence of an external magnetic field, $J_{\rm c}^{\rm S}(H)$. In analogy with the considerations done for the D state [16, 17], the $J_{\rm c}^{\rm S/F}(T)$ values after the application of a magnetic field higher than $H^{\rm sat}$ can be assumed to be equal to the $J_{\rm c}^{S}(T)$ values measured in a given perpendicular field. This field can be interpreted as the equivalent stray field of the F-layer acting on the S-layer, which now will contain two contributions, one due to the electromagnetic coupling, which strongly depends on $M^{\rm rem}$, and another due to the proximity effect. Even though, in general, the superconducting state in F- and S-layers may depend on profile of the exchange field inside the ferromagnet, in our system it is present independently on the magnetic history of the sample (for more details see appendix A). To estimate this equivalent field, the $J_{\rm c}^{S}(H)$ dependence of a single Nb film 30-nm thick has been measured at $T = 4.2$ K (reduced temperature $t = T/T_{\rm c} = 0.58$) in a perpendicular magnetic field, as reported in figure 4. At the same reduced temperature in the OPR state $J_{\rm c}^{\rm S/F} = 9.4 \times 10^9$ A m^{-2} (see figure 2, triangles). The same value is obtained for the single Nb film in a perpendicular field of $H \approx 240$ Oe.

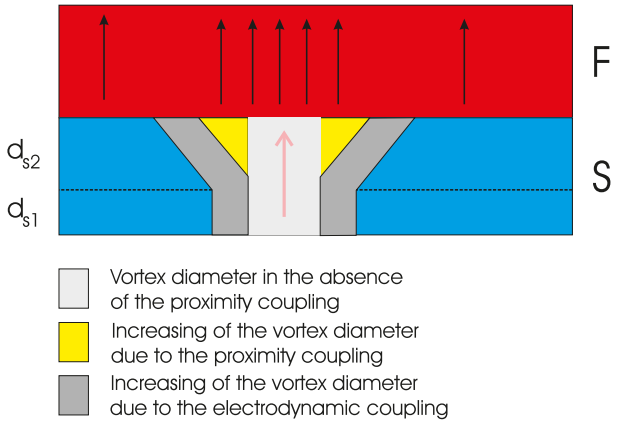

Figure 5. Schematic (not in scale) representation of the magnetic state and vortex dimensions in the Nb/PdNi bilayer when both proximity and electromagnetic coupling are considered. The vortex in the S-layer is induced by the out-of-plane component of the PdNi remanent magnetization. See text for further details.

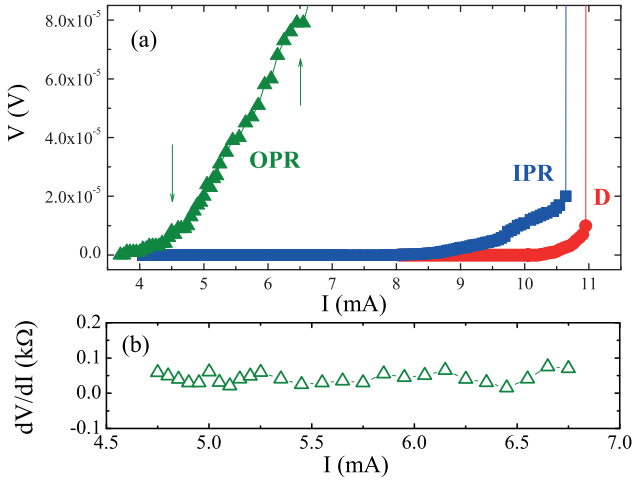

Figure 6. (a): I–V characteristics for the Nb/PdNi bilayer at $T = 4.2$ K. Circles correspond to measurements acquired with the PdNi in the D state. Triangles (squares) correspond to measurements performed in the OPR (IPR) state. Arrows indicate the range in which flux flow is present. (b): differential resistance, $\mathrm{d}V/\mathrm{d}I$, versus I obtained from the part of the I–V curve (OPR state) marked by the arrows in the main panel.

We are reasonably confident to consider this field as the equivalent stray field of the PdNi layer, H^{stray}, which acts on the Nb layer. Moreover, since $H^{\mathrm{stray}} > H_{c1}$, it follows that spontaneous vortices are present in the OPR state. Now, having demonstrated the possible formation of vortices in S, in order to explain the strong reduction of $J_c^{S/F}(T)$ it is necessary to discuss how the vortex topology is affected by both the proximity and the electromagnetic coupling. Since $d_S = 30$ nm $\gg \xi_S$, the proximity coupling in our Nb/PdNi bilayer does not considerably influence the value of T_c [27, 35], but, within a distance smaller than ξ_S from the S/F interface, the superconducting order parameter is depressed. As a consequence, the vortex diameter will become larger close to the S/F interface. This effect was formerly analyzed for S/N hybrids (N = normal metal) [18]. To extend the model to the S/F case we have studied the influence of the proximity coupling on the screening of the S-layer at different distances from the S/F interface considering the Usadel equations for a S/F bilayer in the presence of an external magnetic field. These results are shown in appendix B. On the other hand, due to the electromagnetic coupling the local magnetic inductance in the F-layer increases in correspondence of the position of the vortex. In turn, this local magnetic field additionally suppresses the superconducting correlations in the S-layer. Over these regions the local reduced temperature is enhanced, thus leading to a further increase of the vortex diameter over the whole vortex length, see figure 3. Therefore, taking into account the contribution of both the proximity and electromagnetic coupling, the vortex in the S/F bilayer has a funnel shape, as schematically represented in figure 5. When the Lorentz force exceeds the pinning strength, the funnel-shaped vortex will move as a unique two-dimensional (2D) object[5]. It is reasonable to suppose that, in the absence of defects, as for high-quality superconducting films, the increased vortex diameter produces an enhanced vortex mobility and hence a critical current density depression. The presence of the spontaneous vortex phase is also reflected in the shape of the I–V characteristics. In figure 6(a) we show I–V curves at $T = 4.2$ K for the demagnetized (circles), OPR (triangles) and IPR (squares) states of the F-layer. After the application of the perpendicular field a large portion of the I–V curve shows a constant differential resistance, which is a fingerprint that the sample is in the flux flow regime [19, 33]. For the sake of convenience, in figure 6(b) $\mathrm{d}V/\mathrm{d}I$ has been plotted as a function of I for the current interval marked by arrows in panel (a). This unexpected result, namely the presence of a steady flux flow in the absence of an external magnetic field, can be considered as further confirmation of the presence of a spontaneous vortex phase in the Nb/PdNi bilayer.

4.2. IPR state

When the sample is prepared in the IPR state, the experiment shows that the reduction of $J_c^{S/F}$ with respect to the demagnetized bilayer is relevant only for temperatures lower than $T \approx 5.25$ K, and, in any case, much smaller than in the OPR state. Here some remanent field is oriented parallel to the surface, $M_{\parallel}^{\mathrm{rem}} \approx 0.3 M_{\parallel}^{\mathrm{sat}}$, but, according to the results shown in figure 2, the magnetocrystalline anisotropy of PdNi thin film dominates and it is reasonable to suppose that an out-of-plane component of the magnetization of the PdNi layer is present also in this case. Obviously, this perpendicular component is smaller than the one in the OPR state ($M_{\perp}^{\mathrm{rem}} > M_{\parallel}^{\mathrm{rem}}$, see section 3) but, in principle, we do not know if this remanent field is larger than H_{c1}. However, if we look at the results shown in figure 6 we may exclude the presence of flux flow regime in the IPR state (squares) since the shape of the I–V curve is very similar to the characteristic measured in the D state (circles). This fact can be presumably explained assuming that in the

[5] The criterion to have a 2D vortex is $L_z \gg d_S$, where L_z is the correlation length of the vortex in the out-of-plane direction. In terms of measurable quantities the condition reads $J_c^{1/2} \ll 0.2 B^{1/4} d_S^{-1}$ where J_c is expressed in A m^{-2}, B in T and d_S in nm [36, 37]. For our system this means $d_S \ll 700$ nm.

IPR state there is no spontaneous vortex phase. This last result has important consequences also for the influence of the PE on the $J_c^{S/F}(T)$ suppression. Indeed, if vortices are not nucleated, proximity depresses $J_c^{S/F}(T)$, but only via the reduction of the superconducting order parameter in the S-layer [16, 17].

Finally, the measurement indicated by a cross in figure 2 shows that the behavior of the bilayer is fully reversible. Indeed the critical current density value measured at $T = 4.9$ K after warming the sample at room temperature and cooling it down again without the application of any field matches with the $J_c^{S/F}$ values measured in the D state.

5. Conclusions

The zero field temperature dependence of the critical current density in a Nb/PdNi bilayer was studied before and after the application of an external magnetic field applied either perpendicularly or in the plane of the substrate. In the first case, due to the strong out-of-plane component of the PdNi remanent magnetization a spontaneous vortex phase is formed in the Nb layer. This causes a significant reduction of the $J_c^{S/F}$ values by a factor of two with respect to the case in which PdNi is in the demagnetized state. When the field is applied parallel to the layer, and then removed, the reduction is less pronounced. Finally, when the sample is warmed up above T_{Curie} and cooled down again to $T = 4.9$ K the values of $J_c^{S/F}$ recover those measured in the former demagnetized state. Experiments were interpreted considering the influence of both the proximity and the electromagnetic coupling. Although the latter is the only effect strongly dependent on the magnetic history, the detrimental effect of the PE is also maximum in the OPR state, since in this case it also causes an enhancement of the mobility of the spontaneous vortices. Therefore, it is reasonable to conclude that a system in which the PE is prevented, for instance introducing an extra insulating layer between Nb and PdNi ones, would present a less dramatic reduction of $J_c^{S/F}$ in the OPR state, limiting the efficiency of a possible device based on the presented effect. Indeed, in this respect it is interesting to note that the analyzed bilayer behaves as a nonvolatile superconducting valve, since it can be reversibly switched between a superconductive (ON) to a normal (OFF) state simply by controlling its magnetic history.

Acknowledgments

The work is supported by the Russian Federation Basic Research Foundation, grant no. 14-02-90018 (M Yu K), the Ministry of Education and Science of the Russian Federation, and by Belarusian Foundation for Basic Research, grant no. F14R-020 (SLP). Professor J Aarts is gratefully acknowledged for the $M(H)$ measurements performed at the Kamerlingh Onnes Laboratory in Leiden.

Appendix A. Influence of the exchange field profile in F on the proximity effect

The proximity effect present at the S/F interface investigated in this work weakly depends on the magnetic history of the sample. However, it is necessary to note that, in general, the superconducting state in F- and S-films may depend on the profile of the exchange field inside the ferromagnet, due, for instance to the presence of domain walls [38, 39] or to the misorientation angle between directions of domain magnetic moment if the geometrical size of the domains is comparable with the decay length in the F-film, ξ_F. For instance, if a sharp domain wall is parallel [40] or perpendicular to the S/F interface [41] and the effective geometrical size of a domain is smaller than ξ_F then, in the presence of domains oriented in antiparallel direction, the exchange field averages out and the decay length of superconducting correlations in F becomes close to that of a nonmagnetic (N) metal. Moreover, if magnetic moments of the neighboring domains have non-collinear orientations long-ranged triplet correlations (LRTCs) may arise [40, 42] and they may additionally suppress the s-wave correlations in the structure. In our particular experimental setup we can exclude all these effects. The easy-axis of magnetization oriented perpendicularly to the films plane allows us to assume that, even in the demagnetized state, the magnetic moments of neighboring domains are predominantly collinear thus making a generation of LRTCs in our structures unlikely. Moreover, the size of our domains (around 100×100 nm^2 [28, 30]) is large compared to ξ_F. Both these conditions, considering also that the system is in the dirty limit support the thesis that, according to [42], the decay length in ferromagnetic film is almost the same throughout the domain area, including the neighborhood of the domain wall and the wall itself. On the other hand, calculations show that, even in the most favorable situation for the generation of LRTCs (magnetic moments of the domains are mutually perpendicular), additional suppression of T_c does not exceed 10% of that achieved in a collinear configuration of domain magnetization [43–45]. This is due to the fact that the presence of LRTCs only modifies the pre-exponential factor of the s-wave component in the F material [43, 44]. Taking all this into account we conclude that in our case there is no valuable influence of the magnetic history of the sample on the proximity effect.

Appendix B. Influence of the proximity effect on the vortex topology in S/F bilayers

Here we discuss, depending on the value of E_{ex} in the ferromagnet, the influence of the proximity effect on the screening capacity of the superconductor. We will first derive the main equations and then we will discuss the temperature region far from T_c (section B.1) and close to T_c (section B.2).

Consider a S/F bilayer in external magnetic field, H, oriented perpendicularly to the bilayer surface. We will assume that the conditions of dirty limit are valid for both layers; moreover the superconducting order parameter, Δ, is zero in the F-layer and $H \gg H_{c1}$. The F-layer has single domain magnetic structure with magnetization vector oriented parallel to H.

We align the z-axis in the direction parallel to the magnetic field, and place the origin of the coordinates at the S/F interface. To define the coordinate dependence of the Green function it

is convenient to use the Wigner–Seitz approximation for an elementary vortex cell [46]. Accordingly, the hexagonal unit cell of the vortex lattice is replaced by a circular cell with radius

$$r_S = r_c\sqrt{\frac{H_{c2}}{H}}. \tag{B.1}$$

For a single superconducting film the critical radius, r_c, and the upper critical field, H_{c2}, are determined by the expressions [47]

$$\begin{gathered} r_c = \sqrt{\frac{\Phi_0}{\pi H_{c2}}}, \\ \ln\frac{T}{T_c} + \psi\left(\frac{1}{2} + \frac{T_c\xi_S^2}{Tr_S^2}\right) - \psi\left(\frac{1}{2}\right) = 0. \end{gathered} \tag{B.2}$$

Here $\psi(x)$ is di-gamma function, $\xi_S = (D_S/2\pi T_c)$, and D_S is the diffusion coefficient of the superconductor. This approximation has been previously used in the study of flux flow regimes in superconducting films [48, 49], as well as in the theoretical analysis of the influence of Abrikosov vortices on the properties of tunnel Josephson junctions [50, 51]. To simplify the problem we will additionally assume that Δ and the anomalous Green's functions in S, F_S, and in F, F_F, are small compared to πT, where T is the temperature. Also, $d_S \ll \lambda_\perp$. Under the above assumptions the system of Usadel equations [52] describing the behavior of S/F bilayer in magnetic field has the form [18]

$$\begin{aligned} &\xi_S^2\frac{d^2F_S}{dz^2} + \xi_S^2\frac{d^2F_S}{dr^2} + \xi_S^2\frac{1}{r}\frac{dF_S}{dr} \\ &\quad - (\Omega + \xi_S^2Q^2)F_S = -\Delta, \qquad 0 \le z \le d_S, \end{aligned} \tag{B.3}$$

$$\begin{aligned} &\xi_F^2\frac{d^2F_F}{dz^2} + \xi_F^2\frac{d^2F_F}{dr^2} + \xi_F^2\frac{1}{r}\frac{dF_F}{dr} \\ &\quad - (\tilde{\Omega} + \xi_F^2Q^2)F_F = 0, \qquad -d_F \le z \le 0, \end{aligned} \tag{B.4}$$

$$Q = \frac{1}{r}\left(1 - \frac{r^2}{r_S^2}\right), \tag{B.5}$$

$$\Delta\ln\frac{T}{T_c} + \frac{T}{T_c}\mathrm{Re}\sum_{\Omega=0}^{\infty}\left[\left(\frac{\Delta}{\Omega} - F_S\right)\right] = 0. \tag{B.6}$$

Here $\Omega = (2n+1)T/T_c$ are the Matsubara frequencies, $\tilde{\Omega} = |\Omega| + iE_{ex}\mathrm{sign}(\Omega)/\pi T_c$ and $\xi_F = (D_F/2\pi T_c)^{1/2}$ where D_F is the diffusion coefficient of the ferromagnet. Equations (B.3)–(B.6) should be supplemented by the boundary conditions at the S/F interface ($z = 0$) [53]

$$F_S(0) = F_F(0), \tag{B.7}$$

$$\xi_S\frac{dF_S(0)}{dz} = \gamma\xi_F\frac{dF_F(0)}{dz}. \tag{B.8}$$

Here $\gamma = \rho_S\xi_S/\rho_F\xi_F$, where $\rho_{S(F)}$ is the low-temperature resistivity of the S(F) metal. It is also supposed for simplicity that the S/F interface is fully transparent for incident electrons. At the free interfaces the boundary conditions are

$$\xi_S\frac{dF_S(d_S)}{dz} = 0, \tag{B.9}$$

$$\xi_F\frac{dF_F(-d_F)}{dz} = 0. \tag{B.10}$$

The solution of the problem (B.3)–(B.10) can be found as

$$F_F(r,z) = U_F(z)r\exp\left(-\frac{r^2}{2r_S^2}\right), \tag{B.11}$$

$$F_S(r,z) = U_S(z)r\exp\left(-\frac{r^2}{2r_S^2}\right), \tag{B.12}$$

$$\Delta(r,z) = \Delta_S(z)r\exp\left(-\frac{r^2}{2r_S^2}\right), \tag{B.13}$$

where functions $U_F(z)$, $U_S(z)$, and $\Delta_S(z)$ obey the equations

$$\xi_F^2\frac{d^2U_F(z)}{dz^2} - \kappa_F^2U_F(z) = 0, \qquad \kappa_F^2 = \tilde{\Omega} + \frac{2}{r_S^2}\xi_F^2 \tag{B.14}$$

$$\xi_S^2\frac{d^2U_S(z)}{dz^2} - \kappa_S^2U_S(z) = -\Delta_S(z), \qquad \kappa_S^2 = \Omega + \frac{2}{r_S^2}\xi_S^2 \tag{B.15}$$

$$\Delta_S(z)\ln\frac{T}{T_c} + \frac{T}{T_c}\mathrm{Re}\sum_{\Omega=0}^{\infty}\left[\left(\frac{\Delta_S(z)}{\Omega} - U_S(z)\right)\right] = 0. \tag{B.16}$$

The solution of (B.14) has the form

$$U_F(z) = u_F\cosh\left(\frac{z+d_F}{\xi_F}\kappa_F\right) \tag{B.17}$$

and its substitution into (B.7) and (B.8) gives

$$\xi_S\frac{dU_S(0)}{dz} = \gamma\kappa_FU_S(0)\tanh\frac{d_F\kappa_F}{\xi_F}. \tag{B.18}$$

B.1. Limit of large S-layer thickness, $d_S \gg \xi_{GL}(T)$

For thick superconducting film, $d_S \gg \xi_S$, the boundary problem (B.9), (B.15), (B.16) and (B.18) reduces to the solution of the linearized Ginzburg–Landau (GL) equation

$$\xi_{GL}^2(T)\frac{d^2\Delta_S(z)}{dz^2} + \Delta_S(z) = 0, \tag{B.19}$$

where $\xi_{GL}(T) = \pi\xi_S/2\sqrt{1 - T/T_c}$. Equation (B.19) is supplemented by boundary conditions (B.9) and we have [54]

$$\xi_{GL}(T)\frac{\partial}{\partial z}\Delta_S(0) = b\Delta_S(0), \qquad z = 0, \tag{B.20}$$

$$b = \frac{\sum_{\omega=-\infty}^{\infty}\Omega^{-2}\xi_{GL}(T)\frac{\partial}{\partial z}U_S(0)}{\sum_{\omega=-\infty}^{\infty}\Omega^{-2}U_S(0)}. \tag{B.21}$$

In the limit of large suppression of the superconductivity at $z = 0$ (i.e. close to the S/F interface) at the first order in the parameter $\gamma\sqrt{E}\tanh(\sqrt{E}d_F/\xi_F) \gg 1$ we have

$$\Delta_S(z) = U_S(z) = Bz, \tag{B.22}$$

where B is a constant. At the second order we obtain from (B.18)

$$U_S(0) = B\frac{\xi_S}{\gamma\kappa_F\tanh(\frac{d_F}{\xi_F}\kappa_F)}. \tag{B.23}$$

After the substitution of (B.23) into (B.21) we arrive at

$$b = \frac{\gamma \xi_{GL}(T)}{\xi_S} \frac{\sum_{\omega=0}^{\infty} \Omega^{-2}}{\mathrm{Re} \sum_{\omega=0}^{\infty} \Omega^{-2} \kappa_F^{-1/2} \coth(\frac{d_F}{\xi_F}\kappa_F)}, \quad \text{(B.24)}$$

$$\Delta_S(z) = A \cos\left(\frac{z - d_S}{\xi_{GL}(T)}\right). \quad \text{(B.25)}$$

From equation (B.25) it follows that the order parameter and the amplitude of the Usadel function become smaller when they approach to the S/F interface.

In the opposite limit of small suppression of superconductivity (which is valid when proximity coupling is absent) at $z = 0$ (i.e. close to the S/F interface) at the first order in the parameter

$$\gamma \sqrt{E} \tanh\left(\sqrt{E} d_F/\xi_F\right) \ll 1 \quad \text{(B.26)}$$

we have

$$\Delta_S(z) = U_S(z) = B, \quad \text{(B.27)}$$

where B is a constant. At the second order

$$\xi_S \frac{dU_S(0)}{dz} = \gamma B \kappa_F \tanh\left(\frac{d_F}{\xi_F}\kappa_F\right) \quad \text{(B.28)}$$

resulting in

$$b = \frac{\gamma \xi_{GL}(T)}{\xi_S} \frac{\mathrm{Re} \sum_{\omega=0}^{\infty} \Omega^{-2} \kappa_F \tanh(\frac{d_F}{\xi_F}\kappa_F)}{\sum_{\omega=0}^{\infty} \Omega^{-2}}. \quad \text{(B.29)}$$

B.2. Limit of small S-layer thickness, $d_S \ll \xi_{GL}(T)$

From equation (B.25) and boundary condition (B.20), it follows, in the limit of small γ (equation (B.26)), that, at the first order approximation, the order parameter and the Usadel functions weakly depend on the coordinate, i.e. $\Delta_S(z) \approx \alpha = \text{const}$. To estimate the deviation of the Usadel functions from the constant values at the next order in γ we can find the solution of (B.14)–(B.16) in the form

$$U_S(z) = \frac{\alpha}{\kappa_S^2} + u_S \cosh\left(\frac{z - d_S}{\xi_S}\kappa_S\right). \quad \text{(B.30)}$$

The boundary condition (B.18) gives

$$u_S = -\frac{\gamma \alpha \kappa_F \tanh(\frac{d_F}{\xi_F}\kappa_F)}{\kappa_S^2[\kappa_S \sinh(\frac{d_S}{\xi_S}\kappa_S) + \gamma \kappa_F \tanh(\frac{d_F}{\xi_F}\kappa_F)\cosh(\frac{d_S}{\xi_S}\kappa_S)]}. \quad \text{(B.31)}$$

The expression for the superconducting current circulating around the vortex core, j_S, can be written as

$$j_S(z, r) = \frac{\alpha^2 \Theta(z)}{\pi T_c e \rho_S} S(d_S) r^2 Q(r) \exp\left(-\frac{r^2}{r_S^2}\right), \quad \text{(B.32)}$$

where

$$S(z) = \frac{T}{T_c} \mathrm{Re} \sum_{\omega=0}^{\infty} \frac{1}{\Omega^2 \kappa_S^4} \times \left[1 - \frac{\gamma \kappa_F \tanh(\frac{d_F \kappa_F}{\xi_F})\cosh(\frac{z - d_S}{\xi_S}\kappa_S)}{\kappa_S \sinh(\frac{d_S \kappa_S}{\xi_S}) + \gamma \kappa_F \tanh(\frac{d_F \kappa_F}{\xi_F})\cosh(\frac{d_S \kappa_S}{\xi_S})}\right]^2 \quad \text{(B.33)}$$

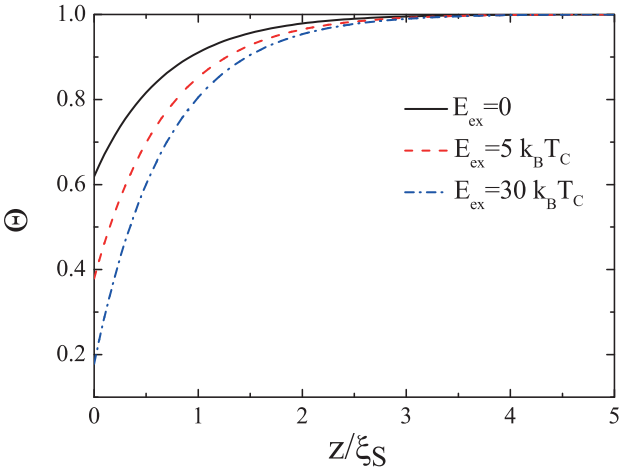

Figure B.1. The parameter Θ from equation (B.32) as a function of the distance from the S/F interface for different values of E_{ex}. $E_{ex} = 0$ corresponds to the S/N case.

and

$$\Theta(z) = \frac{S(z)}{S(d_S)} \quad \text{(B.34)}$$

is the parameter which contains the dependence on the distance from the S/F interface. From equation (B.33) it follows that

$$S(0) = \frac{T}{T_c} \mathrm{Re} \sum_{\omega=0}^{\infty} \frac{1}{\Omega^2} \times \frac{\tanh^2(\frac{d_S}{\xi_S}\kappa_S)}{[\kappa_S \tanh(\frac{d_S}{\xi_S}\kappa_S) + \gamma \kappa_F \tanh(\frac{d_F}{\xi_F}\kappa_F)]^2}. \quad \text{(B.35)}$$

When $d_s \gg \xi_S \kappa_S^{-1}$, it is

$$S(0) \approx \frac{T}{T_c} \mathrm{Re} \sum_{\omega=0}^{\infty} \frac{1}{\Omega^2} \frac{1}{[\kappa_S + \gamma \kappa_F \tanh(\frac{d_F}{\xi_F}\kappa_F)]^2} \quad \text{(B.36)}$$

and

$$S(d_S) \approx \frac{T}{T_c} \sum_{\omega=0}^{\infty} \frac{1}{\kappa_S^2 \Omega^2}. \quad \text{(B.37)}$$

The behavior of $j_S(z)$ is given by the dependence of the parameter $\Theta(z)$ which appears in equation (B.32). The calculated behavior of $\Theta(z)$ for different values of E_{ex} is shown in figure B.1. We see that the screening capacity of Nb significantly decreases when approaching the Nb/PdNi interface.

References

[1] Aladyshkin A Yu, Silhanek A V, Gillijns W and Moshchalkov V V 2009 *Supercond. Sci. Technol.* **22** 053001
[2] Vélez M, Martín J I, Villegas J E, Hoffmann A, González E M, Vicent J L and Schuller I K 2008 *J. Magn. Magn. Mater.* **320** 2547
[3] Buzdin A I 2005 *Rev. Mod. Phys.* **77** 935
[4] Clinton T W and Johnson M J 1998 *J. Appl. Phys.* **83** 6777

Clinton T W and Johnson M J 1999 *J. Appl. Phys.* **85** 1637
[5] Clinton T W and Johnson M 2000 *Appl. Phys. Lett.* **76** 2116
[6] Nadgorny B and Mazin I I 2002 *Appl. Phys. Lett.* **80** 3973
[7] Callegaro L, Ricci S and Vavassori P 2004 *J. Magn. Magn. Mater.* **272–276** e1045
[8] Van de Vondel J, Silhanek A V, Raes B, Gillijns W, Kramer R B G, Moshchalkov V V, Sautner J and Metlushko V 2009 *Appl. Phys. Lett.* **95** 032501
[9] Aladyshkin A Yu and Moshchalkov V V 2006 *Phys. Rev.* B **74** 064503
[10] Zhu L Y, Cieplak M Z and Chien C L 2010 *Phys. Rev.* B **82** 060503(R)
[11] Cieplak M Z, Adamus Z, Kończykowski M, Zhu L Y, Cheng X M and Chien C L 2013 *Phys. Rev.* B **87** 014519
[12] Sonin E B and Felner I 1998 *Phys. Rev.* B **57** R14000
[13] Erdin S, Lyuksyutov I F, Pokrovsky V L and Vinokur V M 2001 *Phys. Rev. Lett.* **88** 017001
[14] Laiho R, Lahderanta E, Sonin E B and Traito K B 2003 *Phys. Rev.* B **67** 144522
[15] Iavarone M, Scarfato A, Bobba F, Longobardi M, Karapetrov G, Novosad V, Yefremenko V, Giubileo F and Cucolo A M 2011 *Phys. Rev.* B **84** 024506
[16] Angrisani Armenio A, Bell C, Aarts J and Attanasio C 2007 *Phys. Rev.* B **76** 054502
[17] Ilyina E A, Cirillo C and Attanasio C 2010 *Physica* C **470** 877
[18] Kupriyanov M Yu 1985 *Fiz. Nizk. Temp.* **11** 1244
Kupriyanov M Yu 1985 *Sov. J. Low Temp. Phys.* **11** 688 (Engl. transl.)
[19] Ryazanov V V, Oboznov V A, Prokofiev A S and Dubonos S V 2003 *Pis. Zh. Eksp. Teor. Fiz.* **77** 43
Ryazanov V V, Oboznov V A, Prokofiev A S and Dubonos S V 2003 *JETP Lett.* **77** 39 (Engl. transl.)
[20] Bell C, Tursucu S and Aarts J 2006 *Phys. Rev.* B **74** 214520
[21] Patiño E J, Bell C and Blamire M G 2009 *Eur. Phys. J.* B **68** 73
[22] Flokstra M, van der Knaap J M and Aarts J 2010 *Phys. Rev.* B **82** 184523 and references therein
[23] Gupta A, Singh G, Kumar D, Kishan H and Budhani R C 2013 *Appl. Phys. Lett.* **103** 182602
[24] Visani C *et al* 2010 *Phys. Rev.* B **81** 94512
[25] Nemes N M, Visani C, Leon C, Garcia-Hernandez M, Simon F, Feher T, te Velthuis S G E, Hoffmann A and Santamaria J 2010 *Appl. Phys. Lett.* **97** 032501
[26] Cirillo C, Ilyina E A and Attanasio C 2011 *Supercond. Sci. Technol.* **24** 024017
[27] Cirillo C, Rusanov A, Bell C and Aarts J 2007 *Phys. Rev.* B **75** 174510
[28] Khaire T S, Pratt W P Jr and Birge N O 2009 *Phys. Rev.* B **79** 094523
[29] Veshchunov I S, Oboznov V A, Rossolenko A N, Prokofiev A S, Vinnikov L Ya, Rusanov A Yu and Matveev D V 2008 *Pis. Zh. Eksp. Teor. Fiz.* **88** 758
Veshchunov I S, Oboznov V A, Rossolenko A N, Prokofiev A S, Vinnikov L Ya, Rusanov A Yu and Matveev D V 2008 *JETP Lett.* **88** 758 (Engl. transl.)
[30] Khasawneh M A, Khaire T S, Klose C, Pratt W P Jr and Birge N 2011 *Supercond. Sci. Technol.* **24** 024005
[31] Jagla E A 2005 *Phys. Rev.* B **72** 094406
[32] Blount E I and Varma C M 1979 *Phys. Rev. Lett.* **42** 1079
[33] Schmidt V V 1997 *The Physics of Superconductors. Introduction to Fundamentals and Applications* ed P Müller and A V Ustinov (Berlin: Springer) p 203
[34] Gubin A I, Il'in K S, Vitusevich S A, Siegel M and Klein N 2005 *Phys. Rev.* B **72** 064503
[35] Mancusi D, Ilyina E A, Kushnir V N, Prischepa S L, Cirillo C and Attanasio C 2011 *J. Appl. Phys.* **110** 113904
[36] Blatter G, Feigelman M V, Geshkenbein V B, Larkin A I and Vinokur V M 1994 *Rev. Mod. Phys.* **66** 1125
[37] Attanasio C, Coccorese C, Maritato L, Prischepa S L, Salvato M, Engel B and Falco C M 1996 *Phys. Rev.* B **53** 1087
[38] Houzet M and Buzdin A I 2006 *Phys. Rev.* B **74** 214507
[39] Volkov A F and Anishchanka A 2005 *Phys. Rev.* B **71** 024501
[40] Volkov A F and Efetov K B 2008 *Phys. Rev.* B **78** 024519
[41] Crouzy B, Tollis S and Ivanov D A 2007 *Phys. Rev.* B **76** 134502
[42] Buzdin A I, Mel'nikov A S and Pugach N G 2011 *Phys. Rev.* B **83** 144515
[43] Fominov Y V, Golubov A A and Kupriyanov M Y 2003 *JETP Lett.* **77** 510
[44] Fominov Y V, Golubov A A, Karminskaya T Yu, Kupriyanov M Y, Deminov R G and Tagirov L R 2010 *JETP Lett.* **91** 308
[45] Zdravkov V I *et al* 2013 *Phys. Rev.* B **87** 144507
[46] Ihle D 1971 *Phys. Status Solidi* b **47** 423
[47] Saint-James D, Sarma G and Thomas E J 1969 *Type II Superconductivity* (Oxford: Pergamon)
[48] Danilov V V, Kupriyanov M Yu and Likharev K K 1974 *Fiz. Tverd. Tela* **16** 935
Danilov V V, Kupriyanov M Yu and Likharev K K 1974 *Sov. Phys.—Solid State* **16** 602 (Engl. transl.)
[49] Kupriyanov M Yu and Likharev K K 1975 *Zh. Eksp. Teor. Fiz.* **68** 1506
Kupriyanov M Yu and Likharev K K 1975 *Sov. Phys.—JETP* **41** 755 (Engl. transl.)
[50] Golubov A A and Kupriyanov M Yu 1986 *Fiz. Nizk. Temp.* **12** 373
Golubov A A and Kupriyanov M Yu 1986 *Sov. J. Low Temp. Phys.* **12** 212 (Engl. transl.)
[51] Golubov A A and Kupriyanov M Yu 1988 *J. Low Temp. Phys.* **70** 83
[52] Usadel K D 1970 *Phys. Rev. Lett.* **25** 507
[53] Kupriyanov M Yu and Lukichev V F 1988 *Zh. Eksp. Teor. Fiz.* **94** 139
Kupriyanov M Yu and Lukichev V F 1988 *Sov. Phys.—JETP* **67** 1163 (Engl. transl.)
[54] Ivanov Z G, Kupriyanov M Yu, Likharev K K, Meriakri S V and Snigirev O V 1981 *Fiz. Nizk. Temp.* **7** 560
Ivanov Z G, Kupriyanov M Yu, Likharev K K, Meriakri S V and Snigirev O V 1981 *Sov. J. Low Temp. Phys.* **7** 274 (Engl. transl.)